

Mechanistic Studies of Olefin Metathesis by Ruthenium Carbene Complexes Using Electrospray Ionization Tandem Mass Spectrometry

Christian Adlhart, Christian Hinderling, Harold Baumann, and Peter Chen*

Contribution from the Laboratorium für Organische Chemie der Eidgenössischen Technischen Hochschule, Zürich, Switzerland

Received October 27, 1999

Abstract: The olefin metathesis reaction of the Grubbs ruthenium carbene complexes has been investigated in the gas phase by electrospray ionization tandem mass spectrometry. Relative rates of reaction for substituted ruthenium benzylidenes and alkylidenes after removal of one phosphine ligand were interpreted with the aid of linear free energy analysis and kinetic isotope effects. The experimental observations are consistent with a reaction profile in which the metallacyclobutane structure is a transition state rather than an intermediate, although alternative explanations cannot be wholly ruled out. Electron withdrawal on the carbene moiety is found to accelerate the metathesis reaction when only the metathesis step itself is examined. Quantum chemical calculations at a variety of levels were performed to check for the consistency of the interpretation.

Introduction

Olefin metathesis is one of the very few, or arguably even the only, fundamentally novel organic transformations discovered in the past four decades. Following the initial report¹ of homogeneously catalyzed metathesis of propylene in 1967, the basic mechanistic picture of the reaction was worked out with contributions from the groups of Calderon, Katz, Casey, Grubbs, Schrock, and others.² The Chauvin mechanism³ via metal carbene complexes has been amply supported by experiment and is now accepted as an accurate depiction of the general course of the reaction. The unique transformation has found considerable application in the Shell higher olefin process (SHOP) for the large-scale production of long-chain α -olefins⁴ and ring-opening metathesis polymerization (ROMP), commercialized by B. F. Goodrich (Telene) and Hercules (Metton) for reaction-injection molding⁵ (RIM), and CDF-Chimie (Norsorex) and Degussa-Hüls (Vestenemer) for specialty resins. The metathesis reaction has furthermore been applied in organic synthesis;⁶ for example, several recent syntheses of a variety of natural and nonnatural products use a ring-closing metathesis to accomplish difficult macrocyclizations.⁷ The recent introduction of well-defined late transition metal metathesis catalysts, particularly ruthenium complexes,^{8,9} has significantly broadened the scope of the reaction due to their substantial tolerance of heteroatom-containing functional groups which had poisoned earlier catalysts. Mechanistic work from the Grubbs group^{10,11}

has elucidated many aspects of the catalytic cycle for this class of metathesis catalyst. With cationized phosphine ligands,¹² a ruthenium benzylidene complex was even rendered soluble and active in water, methanol, or aqueous emulsions.¹³ Despite the wide application of the metathesis reaction, particularly for the new ruthenium carbene complexes, several mechanistic questions remain outstanding. What determines the selectivity in the reaction? What is the rate-determining step? Is the metallacyclobutane an intermediate or transition state? In an earlier report,¹⁴ we used electrospray ionization tandem mass spectrometry (ESI-MS/MS) to investigate the cationized ruthenium carbene complexes in the gas phase.

We report here further mechanistic studies on the (Cy₂RP)-Cl₂Ru=CHAr complex, including isotopic labeling, kinetic isotope effects, and the influence of electron-donating or -withdrawing substituents on the rates of **2** → **3** and **2** → **4** (Scheme 1), which suggest that the metallacyclobutane structure is a transition state rather than an intermediate in the metathesis reaction, at least for the ruthenium carbene complexes. Further

(1) Calderon, N.; Chen, H. Y.; Scott, K. W. *Tetrahedron Lett.* **1967**, 3327.

(2) For several representative reviews spanning the three decades of work, see: Katz, T. J. *Adv. Organomet. Chem.* **1978**, *16*, 283. Calderon, N.; Lawrence, J. P.; Ofstead, E. A. *Adv. Organomet. Chem.* **1979**, *17*, 449. Grubbs, R. H.; Tumas, W. *Science* **1989**, *243*, 907.

(3) Herrison, J. L.; Chauvin, Y. *Makromol. Chem.* **1970**, *141*, 161.

(4) Commercial aspects of olefin metathesis are reviewed in the following: Ivin, K. J.; Mol, J. C. *Olefin Metathesis and Metathesis Polymerization*; Academic Press: New York, 1997; pp 397–410.

(5) Goodall, B. L.; Kroenke, W. J.; Minchak, R. J.; Rhodes, L. F. *J. Appl. Polym. Sci.* **1993**, *47*, 607. McCann, M.; McDonnell, D.; Goodall, B. L. *J. Mol. Catal. A* **1995**, *96*, 31. Rhodes, L. F. European Patent 0 435 146 A2, 1990. Mazany, A. M. European Patent 0 755 938 A1, 1995.

(6) Grubbs, R. H.; Miller, S. J.; Fu, G. C. *Acc. Chem. Res.* **1995**, *28*, 446.

(7) Miller, S. J.; Kim, S. H.; Chen, Z. R.; Grubbs, R. H. *J. Am. Chem. Soc.* **1995**, *117*, 2108. Miller, S. J.; Blackwell, H. E.; Grubbs, R. H. *J. Am. Chem. Soc.* **1996**, *118*, 9606. Fürstner, A.; Langemann, K. *J. Org. Chem.* **1996**, *61*, 3942. Fürstner, A.; Langemann, K. *Synthesis* **1997**, 792. Nicolaou, K. C.; He, Y.; Vourloumis, D.; Vallberg, H.; Yang, Z. *Angew. Chem., Int. Ed. Engl.* **1996**, *35*, 2399. Yang, Z.; He, Y.; Vourloumis, D.; Vallberg, H.; Nicolaou, K. C. *Angew. Chem., Int. Ed. Engl.* **1997**, *36*, 166. Xu, Z.; Johannes, C. W.; Houri, A. F.; La, D. S.; Cogan, D. A.; Hofilena, G. E.; Hoveyda, A. H. *J. Am. Chem. Soc.* **1997**, *119*, 10302. Kamat, V. P.; Hagiwara, H.; Suzuki, T.; Ando, M. *J. Chem. Soc., Perkin Trans. 1* **1998**, 2253.

(8) Nguyen, S. T.; Johnson, L. K.; Grubbs, R. H.; Ziller, J. W. *J. Am. Chem. Soc.* **1992**, *114*, 3974.

(9) Demonceau A.; Noels, A. F.; Saive, E.; Hubert, A. J. *J. Mol. Catal.* **1992**, *76*, 123.

(10) Schwab, P.; Grubbs, R. H.; Ziller, J. W. *J. Am. Chem. Soc.* **1996**, *118*, 100. Ulman, M.; Grubbs, R. H. *Organometallics* **1998**, *17*, 2484.

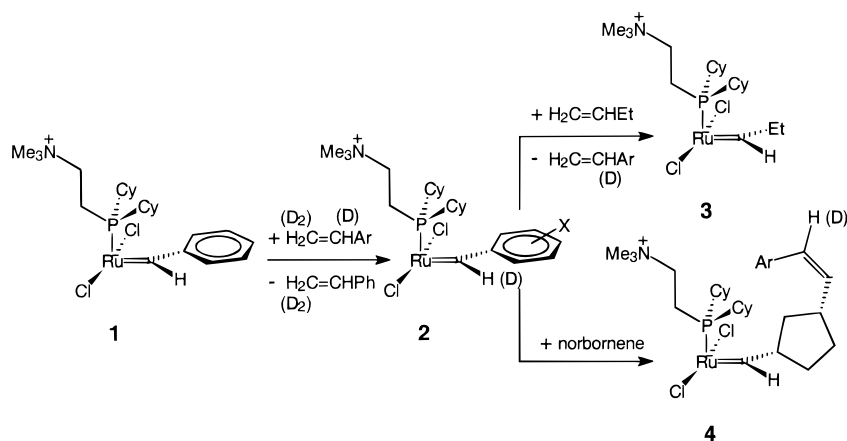
(11) Dias, E. L.; Nguyen, S. T.; Grubbs, R. H. *J. Am. Chem. Soc.* **1997**, *119*, 3887.

(12) Mohr, B.; Lynn, D. M.; Grubbs, R. H. *Organometallics* **1996**, *15*, 4317.

(13) Lynn, D. M.; Mohr, B.; Grubbs, R. H. *J. Am. Chem. Soc.* **1998**, *120*, 1627.

(14) Hinderling, C.; Adlhart, C.; Chen, P. *Angew. Chem.* **1998**, *110*, 2831.

Scheme 1



experiments also directly probe reversibility in the ring-opening metathesis reaction, which had been previously suggested as an important factor in the selectivity of the reaction.

Experimental Section

The monocationic ruthenium benzylidene complex **1** was prepared as previously reported by electrospray of a 10^{-5} M CH_2Cl_2 solution of the dichloride salt of the dicationic bis-phosphine $[(\text{Cy}_2\text{RP})_2\text{Cl}_2\text{Ru}=\text{CHPh}]$. Cy = cyclohexyl, R = 2-(trimethylammonium)ethyl, prepared according to the literature procedure.^{12,13} Mass spectrometric experiments were performed in modified Finnigan MAT TSQ-7000 and TSQ-700 spectrometers as described in earlier papers in this series.^{14,15} The tube lens potential—an indication of the severity of desolvation conditions at the exit of the transfer capillary—was typically kept at 110 V, which was found to be sufficient to both desolvate the electrosprayed ions and furthermore induce loss of one phosphine ligand from the initially produced bis-phosphine, generating **1**. The monophosphine complex **1** was then passed through the first octopole, into which a partial pressure of 10–100 mTorr of a styrene derivative or other olefin had been introduced by a needle valve. Collisions with the olefins served to both thermalize the ions to the 70 °C manifold temperature¹⁶ and induce metathesis to **2**, which was then mass-selected. The subsequent experiments using **2** were performed in daughter-ion mode. The ions **2**, mass-selected in the first quadrupole, were then introduced into the second octopole with a nominal initial kinetic energy of 3 eV (laboratory frame), where they reacted with either acyclic or cyclic olefins, e.g., 1-butene, norbornene, or other substrates (3–5 mTorr). Product ions were then mass-analyzed in the second quadrupole.

The details of the ion–molecule reaction in the second octopole require discussion. In this experiment, the octopole functions more like an ion drift cell, as opposed to a normal collision cell. Monte Carlo modeling (see Appendix), combined with experimental determinations of ion transit times through the octopole, finds that, under the conditions employed in this experiment, the ions undergo up to ~5000 collisions in the second octopole.¹⁴ Moreover, the initial kinetic energy of the ions is lost in the first several collisions. Although there is no applied longitudinal electric field, the continuous ion current into the octopole creates by way of space-charge effects a slight potential that drives the ions through. Based on a comparison of chemical conversion with collision number, the prototype reaction (**1** + butene) \rightarrow (**3** + styrene)

proceeds with an efficiency of between 10^{-4} and 10^{-5} , making it an unusually inefficient ion–molecule reaction even though it is likely to be slightly exothermic. Although normal scans of the second quadrupole are used to check for “cleanliness” of reactions, quantitative data were measured in the segmented-scan mode to achieve a higher signal-to-noise ratio. A single relative rate determination is the average of 15 individual measurements of conversion efficiency, each of which, in turn, is a measurement of **2** reacting with a given substrate followed immediately by a measurement of **1** with the same substrate for normalization. Error bounds on the relative rates were determined from a *t*-distribution by standard statistical methods and represent 95% confidence limits. Because of the broad isotopic pattern in each peak—ruthenium has seven naturally occurring isotopes and each of the two chlorines has two isotopes—a large mass change is needed to get clean differentiation of product ion intensities in the presence of unreacted starting ions. For example, the kinetic isotope effect determinations using **1-d₆**, prepared by reacting **1** with styrene-*d₈*, were performed by selecting the isotopomer of **1-d₆** at *m/z* = 554 for subsequent daughter-ion experiments. While the selected peak does not represent the statistically most abundant isotopomer, it is a peak which should contain no contribution from undeuterated **1**. The particular selection introduces, of course, primary ruthenium and secondary chlorine kinetic isotope effects, but these should be much smaller than the desired secondary deuterium kinetic isotope effects. For the secondary deuterium kinetic isotope effect for the reaction in the reverse direction, **3** was reacted with styrene or styrene-*d₈* (0.3 mTorr) to form **2** with the corresponding level of deuteration. The reaction in this direction was done with a nominal initial kinetic energy for **3** of 2 eV (laboratory frame). A competing loss of trimethylamine from the phosphine ligand of **3** was used as the reference in a competition to determine the rate of metathesis. Assuming that there is no kinetic isotope effect on the trimethylamine loss, the ratio of **2** to [phosphine-NMe₃] in the daughter-ion mass spectrum for collision with styrene versus styrene-*d₈* is a measure of the secondary deuterium kinetic isotope effect for the metathesis reaction in the formally reverse direction. The result given below is again the average of 20 measurements to obtain good statistics.

Ab initio and density functional theory (DFT) calculations were done using the Gaussian 94 program package¹⁷ running on a DEC Alpha AXP 8400 5/300 or HP/Convex Exemplar SPP2000/X-32 computer. All structures were fully optimized without symmetry constraints; vibrational frequencies were found to be positive for all intermediates. Structures optimized as transition-state structures were confirmed to have only one negative frequency. Details from the computational studies are given in the Supporting Information.

(15) Hinderling, C.; Plattner, D. A.; Chen, P. *Angew. Chem.* **1997**, *109*, 272. Hinderling, C.; Feichtinger, D.; Plattner, D. A.; Chen, P. *J. Am. Chem. Soc.* **1997**, *119*, 10793. Feichtinger, D.; Plattner, D. A. *Angew. Chem.* **1997**, *109*, 1796. Feichtinger, D.; Plattner, D. A.; Chen, P. *J. Am. Chem. Soc.* **1998**, *120*, 7175. Kim, Y. M.; Chen, P. *Int. J. Mass Spectrom.* **1999**, *185*–7, 871.

(16) In other work, we have shown that 10 mTorr collision gas in the first octopole is sufficient to completely thermalize the kinetic energy distribution of the electrosprayed ions, as evidenced by the disappearance of any dependence of collision-induced dissociation thresholds on the capillary temperature.

(17) Frisch, M. J.; Trucks, G. W.; Schlegel, H. B.; Gill, P. M. W.; Johnson, B. G.; Robb, M. A.; Cheeseman, J. R.; Keith, T.; Petersson, G. A.; Montgomery, J. A.; Raghavachari, K.; Al-Laham, M. A.; Zakrzewski, V. G.; Ortiz, J. V.; Foresman, J. B.; Cioslowski, J.; Stefanov, B. B.; Nanayakhar, A.; Challacombe, M.; Peng, C. Y.; Ayala, P. Y.; Chen, W.; Wong, M. W.; Andres, J. L.; Replogle, E. S.; Gomperts, R.; Martin, R. L.; Fox, D. J.; Binkley, J. S.; Defrees, D. J.; Baker, J.; Stewart, J. P.; Head-Gordon, M.; Gonzalez, C.; Pople, J. A. *Gaussian 94*, Revision C.3; Gaussian, Inc.: Pittsburgh, PA, 1995.

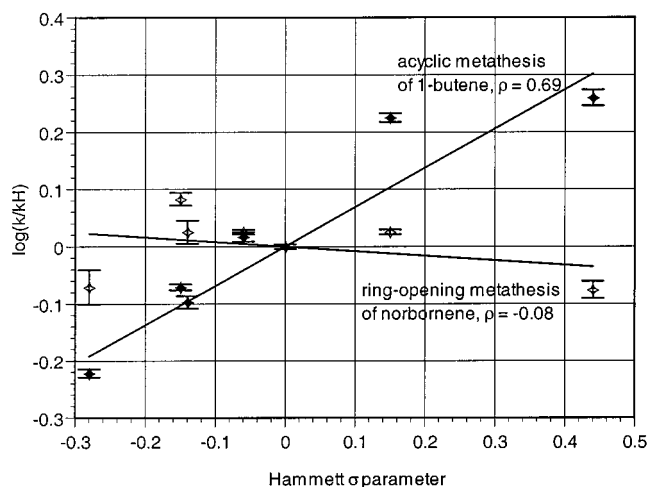


Figure 1. Hammett plots for the relative rate data in Table 1. The solid diamonds represent the reactions with 1-butene; the open diamonds are the reactions with norbornene. A least-squares fit constrained to go through the origin is shown for each series.

Syntheses and characterization of 4-[(Z)-2-pentenyl-3,4,4,5,5,5- d_6]-cyclopentene, 4-[(Z)-2-pentenyl-3,4,4,5,5,5- d_6]-cyclopentane, and 5-vinylnorborn-2-ene¹⁸ are straightforward and are also given in the Supporting Information.

Results

As mentioned in the Introduction, there are several outstanding mechanistic questions in the metathesis reaction catalyzed by ruthenium carbene complexes. Addressing these questions are two kinds of experiments reported in the present work. Relative rate measurements for substituted ruthenium benzylidenes provide the data for kinetic isotope effect and linear free energy relationship analyses. Bifunctional substrates permit an experimental probe of reversibility in ring-opening metathesis. Last, the quantum chemical calculations on the models for species along the reaction coordinate assist in the interpretation of the experimental data, although, as will be seen in the Discussion, it is not altogether clear whether the computed complexes, with PH_3 as a ligand for reasons of computational efficiency, are good models for the actual complexes that have $[(\text{Me}_3\text{NCH}_2\text{CH}_2)\text{PCy}_2]^+$ as a ligand.

Relative Rates and Substituent Effects. Substituted ruthenium benzylidene monophosphine complexes, prepared by reaction of the electrosprayed parent ruthenium benzylidene with a variety of substituted styrenes, react with 1-butene or norbornene with the relative rates shown in Table 1.

Importantly, as reported in our previous communication, norbornene reacts with the parent ruthenium benzylidene monophosphine complex much faster than does 1-butene. A plot of the logarithm of the relative rates for **2** reacting with 1-butene or norbornene against Hammett σ -parameters¹⁹ is linear for both reactions, shown in Figure 1. For the reaction of **2** and 1-butene, $\rho = 0.69 \pm 0.10$, indicating a modest acceleration of the acyclic metathesis reaction by electron-withdrawing groups on the aryl group of the substituted ruthenium benzylidene. For the reaction of **2** and norbornene, on the other hand, $\rho = -0.08 \pm 0.09$, indicating essentially no electronic influence on the rate of the particular ring-opening metathesis reaction.

Moreover, examination of the entries in Table 1 for the reactions of the carbene complex formed from **1** and styrene-

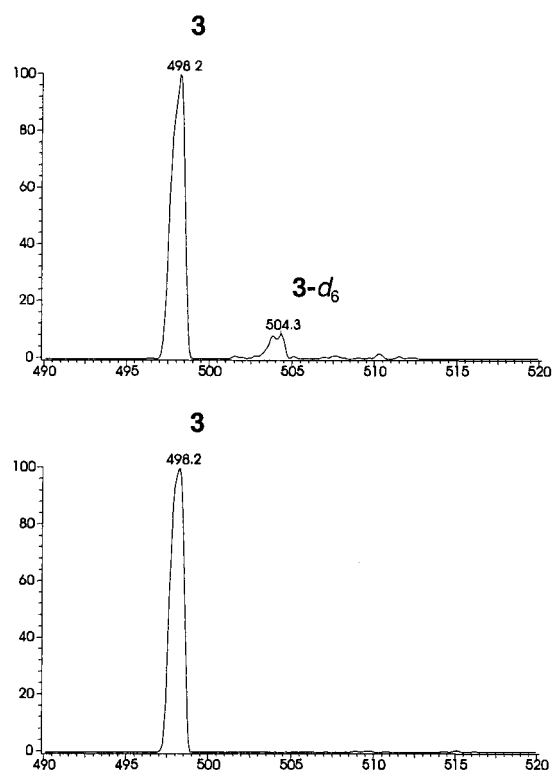


Figure 2. Daughter-ion mass spectra taken by reaction of the mass-selected ruthenium propylidene complex **3**, $m/z = 498$, with 10 mTorr of either 4-[(Z)-2-pentenyl-3,4,4,5,5,5- d_6]-cyclopentene (left-hand spectrum) or 4-[(Z)-2-pentenyl-3,4,4,5,5,5- d_6]-cyclopentane (right-hand spectrum) in the collision cell.

d_8 gives secondary deuterium kinetic isotope effects of $k^H/k^D = 0.80 \pm 0.03$ and 0.96 ± 0.04 for the acyclic metathesis of 1-butene and ring-opening metathesis of norbornene, respectively. The reaction of a ruthenium propylidene complex with styrene, entries 17 and 18 in Table 1, shows a secondary deuterium kinetic isotope effect of $k^H/k^D = 0.86 \pm 0.07$ when the styrene is perdeuterated.

Reversibility in Ring-Opening Metathesis. In our previous communication, we had reported kinetic evidence for the importance of intramolecular π -complexation and reverse reaction in ring-opening metathesis. A more direct test can be made with bifunctional substrates which offer the product of a ring-opening metathesis reaction the chance to undergo a nondegenerate ring-closing metathesis to an isotopically or otherwise substituted complex distinguishable from the original complex by mass.

The cyclopentane derivative does not react with **3** under the relatively mild conditions in this experiment; the cyclopentene derivative, on the other hand, leads to approximately 10% conversion of **3** to **3- d_6** (Scheme 2), as seen in Figure 2, indicating clearly that the ring-opening metathesis of cyclopentene had occurred and is furthermore reversible. While the ring-opening metathesis product of **1** and norbornene can be forced to undergo the reverse reaction regenerating norbornene, harsh conditions—high collision energies, i.e., $\gg 3$ eV in the laboratory frame—are clearly needed to surmount the thermochemical barrier posed by reconstruction of the strained ring. Confirming this is the reaction of **1** with the bifunctional substrate 5-vinylnorborn-2-ene. Acyclic metathesis at the pendant vinyl group produces **5**, while ring-opening metathesis yields either **6** or **7** (Scheme 3). Significantly, no trace of **8** can be seen for conditions used in the relative rate measurements reported in

(18) Ploss, H.; Ziegler, A.; Zimmermann, G. *J. Prakt. Chem.* **1972**, *314*, 467.

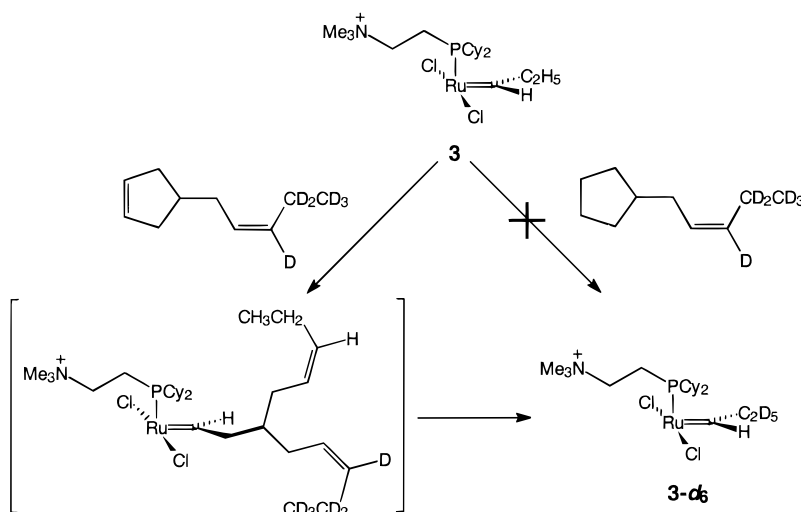
(19) March, J. *Advanced Organic Chemistry*, 4th ed.; Wiley: New York, 1992; p 280.

Table 1. Relative Rates for the Reactions of Ruthenium Carbenes, Determined by Reaction of **1** in the First Octopole with an Olefin, Mass Selection of the Intermediate Carbene in the First Quadrupole, Reaction with an Olefin in the Second Octopole, and Finally Mass Analysis in the Second Octopole^a

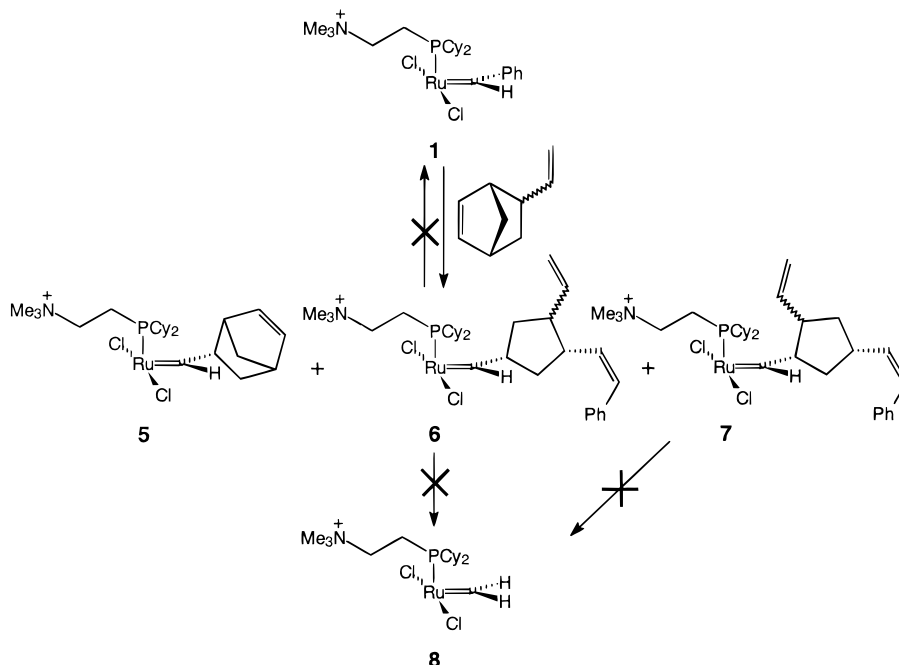
	reagent in O1	selected in Q1	reagent in O2	product in Q2	relative rate
1	<i>p</i> -carbomethoxystyrene		1-butene		1.82 ± 0.06 ^a
2	<i>p</i> -fluorostyrene		1-butene		1.68 ± 0.03 ^a
3	----		1-butene		1.00 ± 0.01 ^a
4	<i>m</i> -methylstyrene		1-butene		1.04 ± 0.02 ^a
5	<i>p</i> -methylstyrene		1-butene		0.80 ± 0.02 ^a
6	<i>p</i> - <i>t</i> -butylstyrene		1-butene		0.85 ± 0.01 ^a
7	<i>p</i> -methoxystyrene		1-butene		0.60 ± 0.01 ^a
8	styrene- <i>d</i> ₈		1-butene		0.80 ± 0.03 ^a
9	<i>p</i> -carbomethoxystyrene		norbornene		0.84 ± 0.03 ^b
10	<i>p</i> -fluorostyrene		norbornene		1.06 ± 0.01 ^b
11	----		norbornene		1.00 ± 0.01 ^b
12	<i>m</i> -methylstyrene		norbornene		1.06 ± 0.01 ^b
13	<i>p</i> -methylstyrene		norbornene		1.06 ± 0.05 ^b
14	<i>p</i> - <i>t</i> -butylstyrene		norbornene		1.21 ± 0.03 ^b
15	<i>p</i> -methoxystyrene		norbornene		1.10 ± 0.01 ^b
16	styrene- <i>d</i> ₈		norbornene		0.96 ± 0.04 ^b
17	1-butene		styrene		1.00 ± 0.03 ^c
18	1-butene		styrene- <i>d</i> ₈		0.86 ± 0.07 ^c

^a Rates are listed relative to that in entry 3 (marked "a"), entry 11 (marked "b"), or entry 17 (marked "c"). Each rate is the average of 15–20 measurements; error bounds are given as 95% confidence bounds based on a *t*-distribution. [Ru] indicates a ruthenium center complete with ligands. For entries 17 and 18, the propylidene complex was prepared in solution rather than in situ.

Scheme 2



Scheme 3



this work, even in segmented-scan mode, placing an upper limit on the amount of **8** at $\ll 0.1\%$.

Quantum Chemical Calculations. Full geometry optimization and calculation of vibrational frequencies were done for all complexes. Several of the species showed multiple non-equivalent minima, so the geometries were intentionally perturbed and then reoptimized to ensure that the global minimum could be identified. (PH₃)₂Cl₂Ru=CH₂ (**9**) is a model for the Grubbs catalyst itself. (PH₃)Cl₂Ru=CH₂ (**10**) represents the species formed after dissociation of one phosphine from **9**. The π -complex of **10** and ethylene, (PH₃)Cl₂Ru=CH₂(η^2 -H₂C=CH₂), is **11**. (PH₃)Cl₂Ru(-CH₂CH₂CH₂-) (**12a** and **12b**) are two isomeric metallacyclobutanes. **12a** is formed directly from **11** through TS₁, while **12b** is formed from **12a** by a pseudorotation through TS₂. Different levels of theory were checked to establish the level needed to obtain reliable results; the best previous calculations used the B3LYP/LANL2DZ method. Broo²⁰ has reported a study of the reliability of various basis

sets for the geometry optimization of ruthenium complexes for which experimental geometries are known. He found that all-electron basis sets were superior to basis sets with effective core potentials (ECPs) and that, furthermore, polarization functions on the ruthenium were needed to reproduce experimental bond lengths. We compared geometries for **10**, computed using the best basis set from Broo (MIDI + 3f on Ru, D95 on PH₃, and D95** on CH₂ and Cl), with that using LANL2DZ and found significant differences. Moreover, we optimized **10** using density functional calculations and compared the geometry to those computed using ab initio methods up to MP4, and we found that B3LYP performed well in comparison to the MP4 calculation. With regard to computational speed, the increase in the number of electrons in the all-electron basis sets (compared to basis sets with an ECP) is more than outweighed by the availability of analytical gradients and second derivatives. Structures, relative energies, and zero-point energies for the complexes **9**–**12** are shown in Figure 3. To place all of the species on a common energy scale, either PH₃ or ethylene is

(20) Broo, A. *Int. J. Quantum Chem. Symp.* **1996**, *30*, 119.

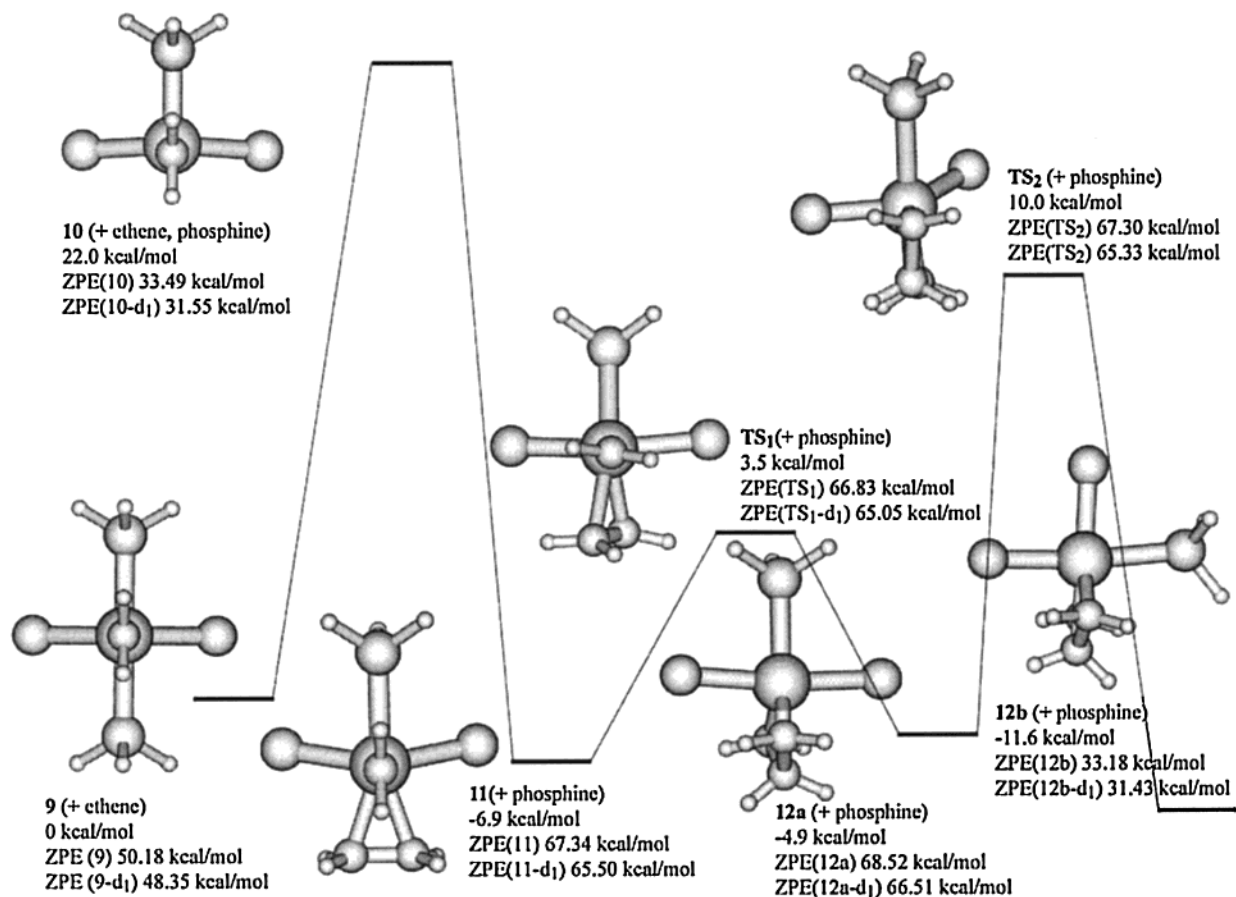


Figure 3. Structures, relative energies, and zero-point energies of complexes **9**–**12** and transition states, **TS₁** and **TS₂**, according to B3LYP calculations with the Broos basis set. Zero-point energies for the deuterated species are given for a single deuteration on the CH₂ unit. All energies are given in kilocalories per mole.

included in the calculation of energy relative to **9** when necessary. Although the calculation places the metallacyclobutane structure **12a** above the π -complex **11**, consistent with the absence of an observable (by NMR) or isolable metallacyclobutane in this reaction, another metallacyclobutane **12b** was found at lower energy.

The isomeric structure could be accessed from **11** only via **12a** and transition state **TS₂**. The latter lies above the transition state **TS₁**, which in a degenerate metathesis reaction is the transition state leading to product. Accordingly, **12b** should be kinetically inaccessible in the reaction.

Discussion

Electrospray ionization tandem mass spectrometry has recently emerged as a powerful tool for mechanistic and analytical studies of organometallic reactions and other catalyzed reactions.^{14,15,21} Nevertheless, for the metathesis reaction by a

catalyst which has been characterized in solution, there has been only the previous report from this group,¹⁴ although the prototype reaction has been studied mass spectrometrically for several simple metal carbenes,²² e.g., [Mn=CH₂]⁺, [Fe=CH₂]⁺, and [Co=CH₂]⁺, mostly by reaction with deuterated ethylene. The questions concerning the role of the various ligands and substitution on those ligands require that the elaborated complex, as close to the solution-phase catalyst as possible, be studied.

In a series of papers, Grubbs and co-workers^{8,10–13} have mapped out much of the important features of the metathesis reaction catalyzed by well-characterized ruthenium carbene complexes. Recent work from other groups^{23–25} has added further to the understanding of the reaction. Although some of the experimental papers have included computational components, there has been only a single full computational paper on the metathesis reaction catalyzed by ruthenium carbene complexes.²⁶ Despite the body of work that has appeared in these reports, there remain outstanding questions, three of which were listed in the Introduction: What determines the selectivity in the reaction? What is the rate-determining step? Is the metallacyclobutane an intermediate or transition state?

(21) Colton, R.; Traeger, J. C. *Inorg. Chim. Acta* **1992**, *201*, 153. Canty, A. J.; Traill, P. R.; Colton, R.; Thomas, I. M. *Inorg. Chim. Acta* **1993**, *210*, 91. Colton, R.; D'Agostino, A.; Traeger, J. C. *Mass Spectrom. Rev.* **1995**, *14*, 79 and references therein. Kane-Maguire, L. A. P.; Kanitz, R.; Sheil, M. M. *J. Organomet. Chem.* **1995**, *486*, 243. Lipshutz, B. H.; Stevens, K. L.; James, B.; Pavlovich, J. G.; Snyder, J. P. *J. Am. Chem. Soc.* **1996**, *118*, 6796. Jiao, C. Q.; Freiser, B. S.; Carr, S. R.; Cassidy, C. J. *J. Am. Soc. Mass Spectrom.* **1995**, *6*, 521. Gatlin, C. L.; Turecek, F. In *Electrospray Ionization Mass Spectrometry*; Cole, R. D., Ed.; John Wiley: New York, 1997; Chapter 15. Dzhabiava, Z. M.; Kozlovskii, V. P.; Shul'ga, Yu. M.; Dodonov, A. F.; Belov, G. P. *Russ. Chem. Bull.* **1996**, *45*, 474. Saf, R.; Schitter, R.; Mirl, C.; Stelzer, F.; Hummel, K. *Macromolecules* **1996**, *29*, 7651. Aliprantis, A. O.; Canary, J. W. *J. Am. Chem. Soc.* **1994**, *116*, 6985. Wilson, S. R.; Wu, Y. *Organometallics* **1993**, *12*, 1478. Alpin, R. T.; Baldwin, J. E.; Schofield, C. J.; Waley, S. G. *FEBS Lett.* **1990**, *277*, 212.

(22) Stevens, A. E.; Beauchamp, J. L. *J. Am. Chem. Soc.* **1979**, *101*, 6449. Jacobson, D. B.; Freiser, B. S. *J. Am. Chem. Soc.* **1985**, *107*, 67. Jacobson, D. B.; Freiser, B. S. *J. Am. Chem. Soc.* **1985**, *107*, 2605.

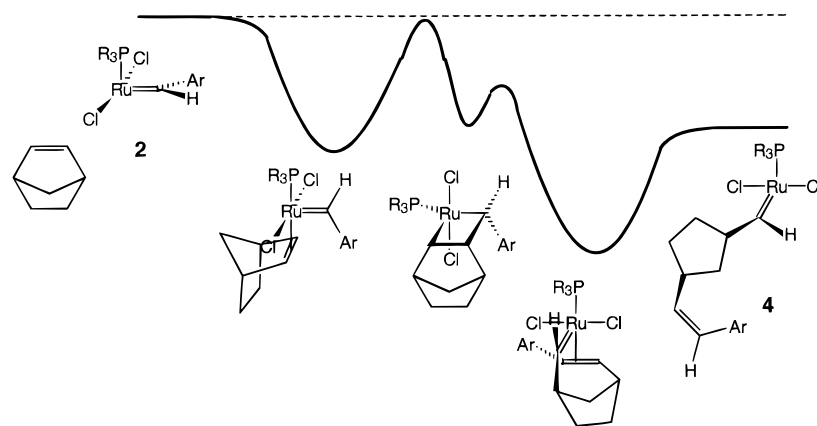
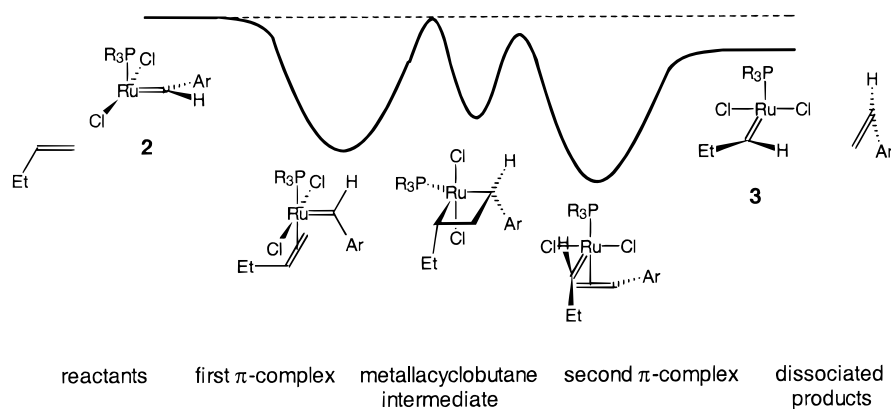
(23) Hansen, S. M.; Rominger, F.; Metz, M.; Hofmann, P. *Chem. Eur. J.* **1999**, *5*, 557.

(24) Hansen, S. M.; Volland, M. A. O.; Rominger, F.; Eisenträger, F.; Hofmann, P. *Angew. Chem.* **1999**, *111*, 1360.

(25) Tallarico, J. A.; Bonitatebus, P. J., Jr.; Snapper, M. L. *J. Am. Chem. Soc.* **1997**, *119*, 7157.

(26) Aagaard, O. M.; Meier, R. J.; Buda, F. *J. Am. Chem. Soc.* **1998**, *120*, 7174.

Scheme 4



In the previous communication,¹⁴ we had argued on kinetic grounds that ring-opening metathesis polymerization (ROMP) of cyclopentene and cyclohexene (in comparison to ROMP of cyclobutene or norbornene), not because the ring-opening metathesis itself was inherently slow, but rather because the facile formation of an intramolecular π -complex, favored for the longer, more flexible spacers derived from cyclopentene and cyclohexene, both introduced an unfavorable preequilibrium and promoted an unproductive ring-closing metathesis. This conjecture finds confirmation in the direct probes for reversible ROM by the substituted cyclopentenes and norbornenes in the present study. The ROM of cyclopentene is readily reversible, while that of norbornene is not. As had been argued by Patton and McCarthy,²⁷ strain release in the substrate is not the principal determinant in all but perhaps one of the several orders-of-magnitude difference in apparent ROMP reactivity of cyclohexene versus norbornene in solution. The easy intramolecular π -complexation—primarily a steric effect—and concomitant ring-closing metathesis are the controlling factors.

Electronic effects on relative rates, on the other hand, are seen in Figure 1. As is evident from the Hammett plot of relative rates versus substituents for the reaction of ruthenium benzylidenes with 1-butene, the reaction is accelerated by electron-withdrawing substituents on the carbene moiety. Qualitative reaction coordinates are depicted in Schemes 4 and 5. The overall topology conforms to the general picture for a bimolecular ion–molecule reaction proceeding via initial complexation.²⁸ While there is no attempt here to quantify the well

depths or barrier heights, the reaction coordinates were constructed with the following considerations:

(1) The reactions $2 \rightarrow 3$ and $2 \rightarrow 4$ are both exothermic, with the latter being much more exothermic than the former.

(2) The ion–dipole complex for the gas-phase reaction is assumed to correspond functionally to the π -complex of the solution-phase reaction.

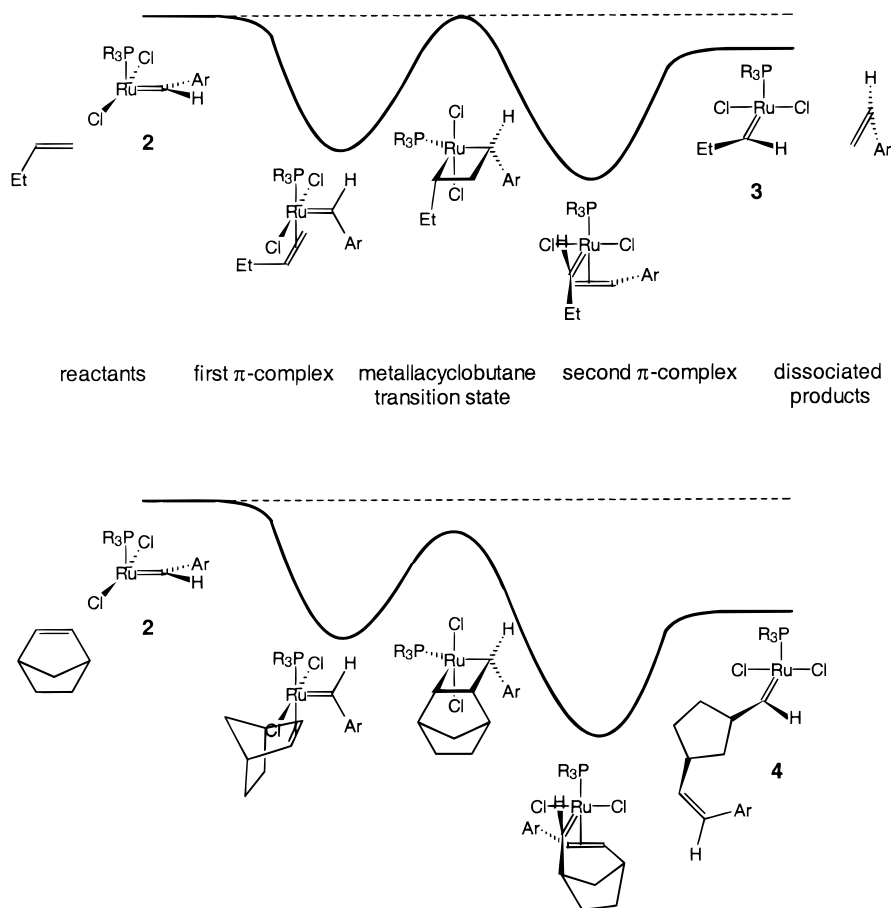
(3) While a solution-phase reaction which proceeded at less than the diffusion-controlled rate would necessarily have a rate-limiting transition state above the entering asymptote, gas-phase ion–molecule reactions with a central barrier (in the conventional double-well potential) below the reactant asymptote can both proceed with less than unit reaction efficiency and display substituent and isotope effects.²⁹ Nevertheless, because the reaction $2 \rightarrow 3$ displays an extraordinarily low reaction efficiency of 10^{-4} – 10^{-5} for an exothermic ion–molecule

(28) Farneth, W. E.; Brauman, J. I. *J. Am. Chem. Soc.* **1976**, *98*, 7891. Olmstead, W. N.; Brauman, J. I. *J. Am. Chem. Soc.* **1977**, *99*, 4219. Asubiojo, O. I.; Brauman, J. I. *J. Am. Chem. Soc.* **1979**, *101*, 3715. Pellerite, M. J.; Brauman, J. I. *J. Am. Chem. Soc.* **1980**, *102*, 5993. Sharma, S.; Kebarle, P. *J. Am. Chem. Soc.* **1982**, *104*, 19. Caldwell, G.; Magnera, T. F.; Kebarle, P. *J. Am. Chem. Soc.* **1984**, *106*, 959. McMahon, T. B.; Heinis, T.; Nicol, G.; Hovey, J. K.; Kebarle, P. *J. Am. Chem. Soc.* **1988**, *110*, 7951.

(29) A particularly well-documented study finds for gas-phase proton-transfer reactions between pyridine bases that even for the case where the central barrier is below the entering asymptote of an exothermic reaction, the reaction efficiency can be on the order of 0.1 with a primary deuterium isotope effect k_H/k_D around 1.4. See: Jasinski, J. M.; Braumann, J. I. *J. Am. Chem. Soc.* **1980**, *102*, 2906. The general theory of kinetic isotope effects—and solution-phase experiments in general—finds primary deuterium isotope effects that are much larger, a typical value being $k_H/k_D = 6$ –8 for proton transfer through a linear transition state. The argument used in the present study—attenuation of substituent and isotope effects when the rate-limiting transition state is pulled well below the entering asymptote—is, in fact, supported by the proton-transfer study.

(27) Patton, P. A.; McCarthy, T. J. *Macromolecules* **1984**, *17*, 2939. Patton, P. A.; McCarthy, T. J. *Polym. Prepr.* **1985**, *26*, 66. Patton, P. A.; McCarthy, T. J. *Macromolecules* **1987**, *20*, 778.

Scheme 5



reaction, the rate-determining transition states in the upper panels of Schemes 4 and 5 have been depicted (for convenience) to lie at roughly the level of the entering asymptote.³⁰ This is not meant, however, to imply a quantitative assessment.

(4) The Hammond Postulate is assumed to be valid.

Within this framework, the particular direction of the substituent effect is easily rationalized if one proceeds from the assumption that the ruthenium center in **1** is electron-deficient and is accordingly destabilized by electron-withdrawing substituents on the benzylidene fragment. The aryl group on the corresponding metallacyclobutane is, however, no longer in direct conjugation to the ruthenium. By this logic, the metallacyclobutane, and any putative transition state leading to it from a carbene complex, is destabilized less by electron withdrawal than either the carbene or the carbene/olefin π -complex would be, leading to a moderately large, positive Hammett ρ value. This would necessarily make rate-determining that transition state in which a metallacyclobutane structure is formed. Furthermore, the secondary deuterium kinetic isotope effect in the forward direction, $k^H/k^D = 0.80 \pm 0.03$, considered in the usual way, indicates an $sp^2 \rightarrow sp^3$ transition going to the rate-

determining transition state, which is also consistent with the assignment of the rate-determining step for the gas-phase reaction **2** \rightarrow **3**.

Either the two-step metathesis reaction **2** \rightarrow **3** depicted in Scheme 4 (upper trace) or the one-step reaction depicted in Scheme 5 (upper trace) would be consistent with the substituent and (forward direction) isotope effect. If the two-step reaction were to be correct, as is usually assumed, one can also argue that, for the reaction **2** \rightarrow **3**, metallacyclobutane formation in the upper trace in Scheme 4 must be rate-determining because the acyclic metathesis reaction is merely a slightly perturbed degenerate reaction, which when slightly exothermic as postulated above places the first transition state higher than the second. The distinction comes from the comparison with **2** \rightarrow **4**, which, in contrast, shows neither an electronic substituent effect nor a secondary deuterium kinetic isotope effect and provides the first clue to the rate-determining step in the reaction. The difference in ρ cannot be due to reversibility in the ring-opening metathesis, because, although ROM of cyclopentene goes both ways under the present conditions, the probe with 5-vinylnorborn-2-ene clearly rules out reversibility except under forcing conditions for the ROM reaction of norbornene.

The principal difference relevant to the two different ρ values is the different exothermicities of the acyclic metathesis of 1-butene versus the ring-opening metathesis of norbornene. We expect the gas-phase reaction of **2** \rightarrow **3** to be mildly exothermic because, as Grubbs noted,¹⁰ an alkyl group is both smaller and more electron-donating than a phenyl and, accordingly, should stabilize the ruthenium center. The ring-opening metathesis of norbornene, **2** \rightarrow **4**, should be much more exothermic because, in addition to the electronic and steric factors, the strain release

(30) The observed secondary deuterium isotope effect for the acyclic metathesis reaction **2** \rightarrow **3** is not attenuated at all relative to expectations from theory or solution-phase studies, while that for the ROM reaction **2** \rightarrow **4** has been completely washed out. The qualitative surfaces in Schemes 4 and 5 correspond to potential energy surfaces. Inclusion of entropy—or, equivalently, transformation to free energy surfaces—would raise the transition states more than the entering asymptote because of the loss of translational and rotational entropy in the formation of a complex from two components. A quantitative treatment with RRKM theory is not possible because the real complexes are too large for a reasonable level of quantum chemical theory to calculate reliable frequencies. Nevertheless, the important comparison—the reaction of **2** \rightarrow **3** versus **2** \rightarrow **4**—can be made without recourse to quantitative rates.

upon cleavage of the olefinic linkage in norbornene should add approximately 15 kcal/mol to the reaction exothermicity.³¹ If the increased reaction exothermicity, by the Hammond postulate, were to pull whichever transition state was rate-limiting to an energy well below the starting point of the reaction, then both electronic substituent effects and the secondary deuterium kinetic isotope effect should be greatly attenuated. In either Scheme 4 or 5, the thermochemistry going from the carbene and norbornene to the first π -complex should not be too different from that in the corresponding step in acyclic metathesis because little of the strain in norbornene is released by π -complexation.³² Likewise, formation of the metallacyclobutane releases little strain if the metallacyclobutane is a bound intermediate, as assumed in Scheme 4. Strain release should, however, greatly lower the transition state for metallacyclobutane cleavage in Scheme 4, which nevertheless does not affect the preceding rate-determining transition state. This argues against Scheme 4 as a description of the reaction coordinate for the gas-phase metathesis reactions of **2**. On the other hand, Scheme 5 shows the reaction coordinate for a one-step reaction, i.e., metallacyclobutane as transition state. By Hammond's postulate, the rate-determining transition state will be pulled down by the strain release on going from reactant to product. Supporting the argument is the isotope effect on the acyclic metathesis reaction, going in the opposite direction. Entries 17 and 18 in Table 1 clearly indicate that $k^H/k^D = 0.86 \pm 0.07$ for the reaction $([\text{Ru}] = \text{CHEt} + \text{styrene}) \rightarrow ([\text{Ru}] = \text{CHPh} + 1\text{-butene})$. Typically, the only way that an acyclic metathesis reaction of a ruthenium benzylidene complex and an α -olefin could show a substantial³³ inverse secondary deuterium kinetic isotope effect in both the forward and reverse directions would be if Scheme 5 described the reaction coordinate. We note also that no ion corresponding in mass to the metallacyclobutane could be observed in any of the acyclic metathesis experiments. A single, published computational study of the entire metathesis reaction for a ruthenium carbene complex in solution finds no intermediate at the metallacyclobutane structure,²⁶ in agreement with the current experimental results.

The present computational results find, in contrast to the arguments above, a minimum at the metallacyclobutane structure. Single-point energy calculations at the optimized critical points with the CCSD(T) method find only small changes in the relative energies. Nevertheless, the computation—the best that can be done in the present circumstances—does have problems. The prediction that **9** lies far above all of the other species and, moreover, far above all of the transition states would suggest that the experimentally determined rate of metathesis by **2** should be close to the collision rate. Quantitative measurement of the rate for the acyclic metathesis of 1-butene by **2** finds that the acyclic metathesis rate is lower than the collision rate by between 4 and 5 orders-of-magnitude (vide infra). The most important difference between the computed structures **9–12** and the measured complexes **2–4** is the phosphine. The Tolman cone angles of PH_3 and PCy_3 are 87°

(31) The strain release upon cleavage of one ring of norbornene in a ROM reaction can be estimated from exothermicity of the homodesmotic equation: $(2 \times \text{ethane}) + \text{norbornene} \rightarrow \text{cis-1,3-dimethylcyclopentane} + \text{Z-2-butene}$.

(32) It has been argued that while there is a difference in the π -complexation of norbornene versus cyclopentene with an unsaturated tungsten carbene, the difference is not large. Ivin, K. J.; Lapienis, G.; Rooney, J. J. *Makromol. Chem.* **1982**, *183*, 9. Also, the heats of hydrogenation of ethylene and norbornene are surprisingly similar.

(33) A two-step endothermic reaction (the reverse reaction) would show an overall kinetic isotope effect that is the product of a normal equilibrium isotope effect on the reversible first step and an inverse kinetic isotope effect on the rate-determining second step. The two would largely cancel.

and 170° , respectively.³⁴ The phosphine in complexes **2–4** is accordingly much more sterically demanding than PH_3 (in the calculations), which would destabilize any complex in which any of the other ligands are in van der Waals contact with the phosphine. One could suggest that the very large phosphine changes the reaction coordinate sufficiently that the computed path, shown in Figure 3, does not describe the experimentally studied reaction. An alternative explanation would be that substituent effects and isotope effects for what is effectively a chemically activated gas-phase reaction function differently from those in thermal reactions in solution, where each intermediate is thermalized before proceeding to the next step. A similar situation had been suggested for the multistep formation of benzene in flames.³⁵ Further computational studies are needed to clarify the issues.

Interestingly, if the structures **9–12**, TS_1 , and TS_2 are simply taken as such, without regard to computed relative energies, one can compute secondary deuterium kinetic isotope effects for the reactions according to Scheme 4 or 5 using the calculated zero-point energies. Using an admittedly crude model, eq 1, one needs only frequencies for each structure to get the isotope effects on an elementary reaction step.³⁶ Using $T = 343 \text{ K}$ and

$$k^H/k^D \approx \frac{\prod_i^{\text{transition-state modes}} \exp\left[-\frac{1}{2}\left(\frac{h\nu_{iH}^{\text{ts}}}{kT} - \frac{h\nu_{iD}^{\text{ts}}}{kT}\right)\right]}{\prod_j^{\text{reactant modes}} \exp\left[\frac{1}{2}\left(\frac{h\nu_{jH}^{\text{r}}}{kT} - \frac{h\nu_{jD}^{\text{r}}}{kT}\right)\right]} \quad (1)$$

the zero-point energies in Figure 3, we find for three hypothetical reactions, kinetic isotope effects of $k^H/k^D = 1.09$ for $\mathbf{11} \rightarrow [\text{TS}_1]^\ddagger \rightarrow \mathbf{12a}$, $k^H/k^D = 1.42$ for $\mathbf{12a} \rightarrow [\text{TS}_1]^\ddagger \rightarrow \mathbf{11}$, and $k^H/k^D = 0.77$ for $\mathbf{11} \rightarrow [\mathbf{12a}]^\ddagger \rightarrow \mathbf{11}$. For the last of the three reactions, the calculation was made assuming that **12a** was a transition state as in Scheme 5. Accordingly, the two-step mechanism in Scheme 4 should show a small normal isotope effect if the first step is rate-determining. Even if the two transition states in the top panel of Scheme 4 were close enough in energy so that neither is clearly rate-determining, the symmetry of the reaction coordinate would reduce the overall kinetic isotope effect to something like that for $\mathbf{11} \rightarrow [\text{TS}_1]^\ddagger \rightarrow \mathbf{12a}$. The experimental result does not agree with this prediction. On the other hand, the calculation of the expected isotope effect for the reaction according to the reaction, $\mathbf{11} \rightarrow [\mathbf{12a}]^\ddagger \rightarrow \mathbf{11}$, yields an inverse isotope effect of the same magnitude as seen in the experiment, again suggesting that the metallacyclobutane is a transition state. One should be careful not to make too much of this last result—if, in fact, the reaction coordinate is substantially altered by a sterically demanding phosphine, then the agreement with experiment derives from only the general trends accompanying hybridization changes.

Can these gas-phase results be reconciled with the solution-phase reactivity studies by Grubbs? While the solution-phase studies of the ruthenium carbenes with Cl, Br, I, acetate, or trifluoroacetate on the metal center indicated increased metathesis activity with electron withdrawal,¹¹ consistent with the present Hammett analysis, the effect was explained as a *trans-*

(34) Collman, J. P.; Hegedus, L. S. *Principles and Applications of Organotransition Metal Chemistry*; University Science Books: Mill Valley, CA, 1980; p 58.

(35) Stein, S. E.; Walker, J. A.; Suryan, M. M.; Fahr, A. *23rd Symposium (International) on Combustion*; The Combustion Institute: Pittsburgh, PA, 1990; pp 85–90.

(36) Lowry T. S.; Richardson, K. S. *Theory and Mechanism in Organic Chemistry*, 2nd ed.; Harper & Row: New York, 1981; Chapter 2.

effect on the initial ligand exchange equilibrium. On the other hand, investigation of the metathesis reaction of ruthenium benzylidenes, in this case with substitution on the aryl group of either the carbene or the styrene substrate, found no clearly interpretable electronic substituent effects in solution.¹⁰ As seen above, the metathesis reaction of the ruthenium benzylidene monophosphine complex is accelerated by electron withdrawal on the benzylidene moiety. In solution, there is a ligand exchange preceding this step in which one phosphine ligand must first dissociate, and a further ligand exchange at the end of the reaction after metathesis has occurred.^{10,11} The first ligand exchange enters into the overall solution-phase rate as a multiplicative factor, in the case that it is a preequilibrium, and is adversely affected by electron withdrawal on the benzylidene. Accordingly, the two effects run in opposite directions, making the overall solution-phase electronic substituent effect ambiguous. Both electron withdrawal and electron donation on the ruthenium benzylidene were reported¹⁰ to decrease the rate of metathesis by $(\text{C}_3\text{P})_2\text{Cl}_2\text{Ru}=\text{CHAr}$, which is understandable if the effect on the ligand exchange dominates for electron-withdrawing groups while the effect on the metathesis step itself dominates for electron donors. The secondary deuterium kinetic isotope effect, $k^{\text{H}}/k^{\text{D}} = 1.7$, observed by Grubbs and co-workers¹⁰ for the reaction $(\text{C}_3\text{P})_2\text{Cl}_2\text{Ru}=\text{CHPh} + \text{styrene-}d_8$, could likewise be attributed to a composite of three effects: the kinetic isotope effect for the metathesis reaction itself and two partition isotope effects³⁷ for the ligand exchanges prior to and following the metathesis.

Conclusion

Gas-phase mechanistic studies of the olefin metathesis by ruthenium benzylidene complexes by way of electronic substituent effects, kinetic isotope effects, suggest that the putative metallacyclobutane structure is a transition state rather than an intermediate. Quantum chemical calculations indicate that there are multiple, delicately balanced effects that need to be considered. The gas-phase study, which avoids the solution-phase problem of prior and subsequent ligand exchange reactions, can nevertheless be reconciled with the solution-phase results in a way that deconvolutes the various contributions to the solution-phase chemistry.

Acknowledgment. Support of this project by the Forschungskommission der Eidgenössischen Technischen Hochschule Zürich, the Schweizerischer Nationalfonds zur Förderung der wissenschaftlichen Forschung, and a graduate fellowship for C.H. from the Stipendienfonds der Basler Chemischen Industrie is acknowledged.

Appendix 1

The Monte Carlo modeling of ion motion in a gas-filled radio frequency multipole ion guide was done as follows. The differential equations for the ion motion in an ideal multipole field were solved numerically without recourse to the effective potential approximation using a fourth-order Runge-Kutta numerical integration. Collisions were handled in a simplified manner. The probability of a collision between the ion and a buffer gas molecule during a single integration time step was treated using Langevin theory:

$$P = nv\sigma = \frac{e}{2\epsilon_0} \sqrt{\frac{\alpha_c}{\mu}} \frac{p}{kT}$$

where P is the collision probability; n is the gas number density;

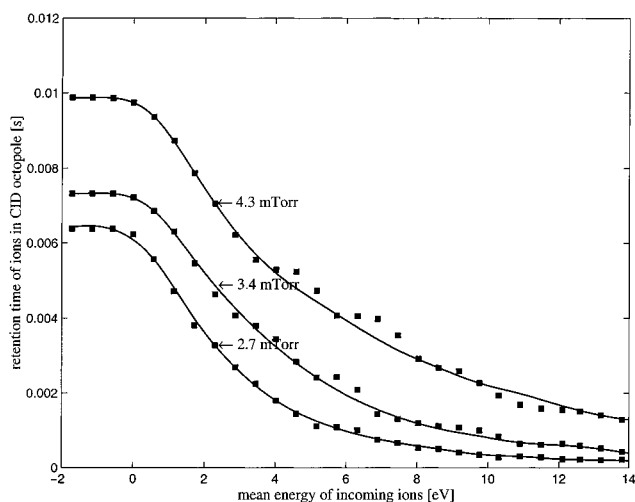


Figure 4. Simulation of the mean ion retention time in the gas-filled octopole collision cell as a function of incident ion energy and gas pressure for the reaction of ruthenium benzylidene complex **1** with 1-butene. The results at nominally negative incident ion energies come from the high-energy tail of the ion kinetic energy distribution.

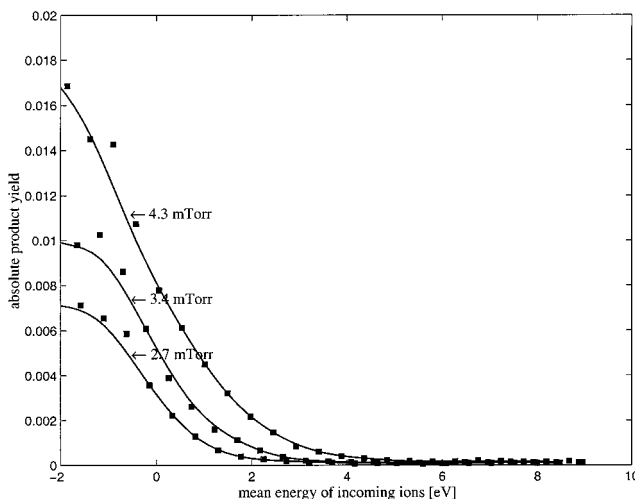


Figure 5. Absolute product yields for the reaction **1** and 1-butene as a function of the incident kinetic energy of **1** (laboratory frame) and the pressure of 1-butene in the octopole collision cell.

v is the relative velocity; σ is the Langevin collision cross section; p is the gas pressure; e is the elementary charge; μ is the reduced mass; ϵ_0 is the electrical permittivity of vacuum; α_c is the polarizability; k is Boltzmann's constant; and T is the absolute temperature.

The application of Langevin theory for the collision cross section greatly simplifies the calculation because, at this level of approximation, the collision probability during a time step is independent of the relative velocities of the collision partners in the center-of-mass frame.

The velocity of the collision partner is taken from a Boltzmann distribution with a random direction in the laboratory frame of reference. For a collision the new direction of the ion is chosen at random in the center-of-mass frame of reference and then transformed back to the laboratory frame. This is equivalent to having chosen a random impact parameter for the collision. In Figure 4, the results of the simulation for three pressures and a range of incident kinetic energies (laboratory frame) are depicted. A test as to whether the simulation gave realistic results was done by sending an ion of a given mass through the first quadrupole, the octopole collision cell, and

the second quadrupole. The two quadrupoles were scanned with a variable time delay between them. By measuring the transmitted ion intensity as a function of the delay between the two quadrupoles, the mean retention time in the octopole could be determined. It was found to agree within a factor of 2 with the simulation. Absolute reaction yields for the metathesis reaction at the same incident ion energies and 1-butene pressures could also be measured.

The plots of measured yield against the same pressure and incident energy parameters are shown in Figure 5. Because the Monte Carlo simulation realistically reproduces the experimentally determined retention time of the ions in the gas-filled octopole, the absolute collision number from the simulation,

up to ~ 5000 collisions per ion, can be taken as reliable. Furthermore, because the curves in Figures 4 and 5 are approximately parallel, one can reduce the measured product yield to a probability of reaction per collision of between 10^{-4} and 10^{-5} .

Supporting Information Available: Geometries, energies, and frequencies for **9–12**, as well as **TS₁** and **TS₂** from the ab initio calculations, and the synthetic details and physical characterization of the several compounds prepared in this study (PDF). This material is available free of charge via the Internet at <http://pubs.acs.org>.

JA9938231